

results do not shed any direct light on this controversy), Armakolas and Klar carried their supposition one step further: If the factors that influence segregation of DNA strands are the same factors that influence left-right body axis formation, then how might a gene product that influences body axis formation influence the segregation of chromatids? They focused on the gene encoding the left-right dynein motor protein (LRD). Mutations in the mouse gene (*Dnahc11*) and the human homolog (*DNAH11*) encoding this motor protein cause left-right axis randomization of some internal organs.

When Armakolas and Klar used the same *Hprt*-recombination experimental system, and reduced expression of the left-right dynein motor by RNA interference, chromatid segregation became nearly “random” in those cell lines in which it had been exclusively the X or Z type. All three cell lines reverted to predominantly the X segregation pattern regardless of whether they were 100% X (embryonic stem cells and endoderm cells) or 100% Z (neuroectoderm cells) in the first place. This segregation ratio (2:1 to 3:1 X:Z segregants) in the absence of LRD is the same as that observed in cell lines that do not normally express LRD (pancreatic cells, mesoderm cells, and cardiomyocytes) and approximately the same as that reported for other embryonic stem cell lines (5) for which the status of LRD expression is unknown. Interestingly, this X:Z segregant ratio is also observed in the fruit fly *Drosophila melanogaster* (6).

One explanation for this ratio is that segregation of *Hprt*-recombinant chromatids presents a topological problem with a single solution (X segregation). Apparent instances of Z segregation are thought to arise as a result either of recombination that normally occurs before DNA replication or of recombination between homologs and between sister chromatids followed by X segregation. The most perplexing observation is not what happens in the absence of LRD but why the presence of LRD leads to exclusive X or Z segregation. What could LRD be doing?

There are at least two possibilities. In neuroectoderm cells, LRD could eliminate *Hprt*-recombination in the G2 phase of the cell division cycle, which is just before the onset of mitosis (but after DNA replication has occurred). On the other hand, in embryonic stem cells and endoderm cells, LRD could eliminate *Hprt*-recombination during the G1 phase, which is before DNA replication begins. This explanation requires only that LRD have a strong negative effect on recombination but does so at different times

during the cell cycle in different types of cells.

The second possibility is that LRD directly affects the orientation of the joined homologs on the spindle, placing the *Hprt*-recombinant chromatids on opposite sides of the metaphase plate (the region of the mitotic spindle where replicated chromosomes are positioned before separation of chromatids into daughter cells) in embryonic stem cells and endoderm cells (X segregation) or on the same side of the metaphase plate (Z segregation) in neuroectoderm cells. It is unclear how LRD might play such a chromosome-orientation role and how the decision on which orientation to take could be based on strand identity. Nevertheless, it is suspicious that a dynein motor protein—a family whose members are involved in chromosome movement—affects chromatid segregation.

Regardless of how this phenomenon is

ultimately explained, Armakolas and Klar are to be commended for testing an unorthodox hypothesis by an experiment that was not an obvious approach. Major scientific discoveries are rarely accompanied by investigators shouting “eureka” but are often accompanied by investigators mumbling “that’s strange.” At first sight, I confess I thought it a strange result.

References

1. A. Armakolas, A. J. S. Klar, *Science* **315**, 100 (2007).
2. J. Cairns, *Nature* **255**, 197 (1975).
3. A. J. S. Klar, *Trends Genet.* **10**, 392 (1994).
4. A. Armakolas, A. J. S. Klar, *Science* **311**, 1146 (2006).
5. P. Liu, N. A. Jenkins, N. G. Copeland, *Nat. Genet.* **30**, 66 (2002).
6. K. J. Beumer, S. Pimpinelli, K. G. Golic, *Genetics* **150**, 173 (1998).
7. J. E. Haber, *Science* **313**, 1045b (2006).

10.1126/science.1137587

PHYSICS

Negative Refractive Index at Optical Wavelengths

Costas M. Soukoulis, Stefan Linden, Martin Wegener

Metamaterials are designed to have structures that provide optical properties not found in nature. If their capacity can be extended, new kinds of devices for imaging and control of light will be possible.

Although discovered only 6 years ago, negative refractive index materials (NIMs) have been the target of intense study, drawing researchers from physics, engineering, materials science, optics, and chemistry. These artificial “metamaterials” are fascinating because they allow the design of substances with optical properties that simply do not occur in nature (1–4). Such materials make possible a wide range of new applications as varied as cloaking devices and ultrahigh-resolution imaging systems. The variety of possible applications would be even greater if such materials could be engineered to work at optical wavelengths.

For the ultimate control of light, one needs a handle on both the electric and the magnetic components of the electromagnetic

(EM) light wave. To achieve this control, normally one would think about modifying the microscopic electric and magnetic fields in a material. However, in most cases it is easier to average over the atomic scale and consider the material to be a homogeneous medium characterized by the electric permittivity ϵ and the magnetic permeability μ . These two quantities describe the EM response of a given material. More specifically, Veselago showed nearly 40 years ago (5) that the combination $\epsilon < 0$ and $\mu < 0$ leads to a negative refractive index, $n < 0$. This means that the phase velocity of light is negative; in other words, light waves now have a “reverse gear.”

Veselago’s idea remained obscure because no such natural materials were known to exist at any frequency. Although electric resonances with $\epsilon < 0$ do occur up to the visible and beyond, magnetic resonances typically die out at microwave frequencies. Moreover, the electric and magnetic resonances would need to overlap in frequency, which seemed improbable. However, by making use of artificially structured metamaterials, in which inclusions smaller than a

C. M. Soukoulis is at the Ames Laboratory and Department of Physics and Astronomy, Iowa State University, Ames, IA 50011, USA, and at the Institute of Electronic Structure and Laser, Foundation for Research and Technology—Hellas, 71110 Heraklion, and the University of Crete, 71409 Heraklion, Crete, Greece. S. Linden and M. Wegener are at the Center for Functional Nanostructures, Universität Karlsruhe and Forschungszentrum Karlsruhe, D-76128 Karlsruhe, Germany. E-mail: soukoulis@ameslab.gov

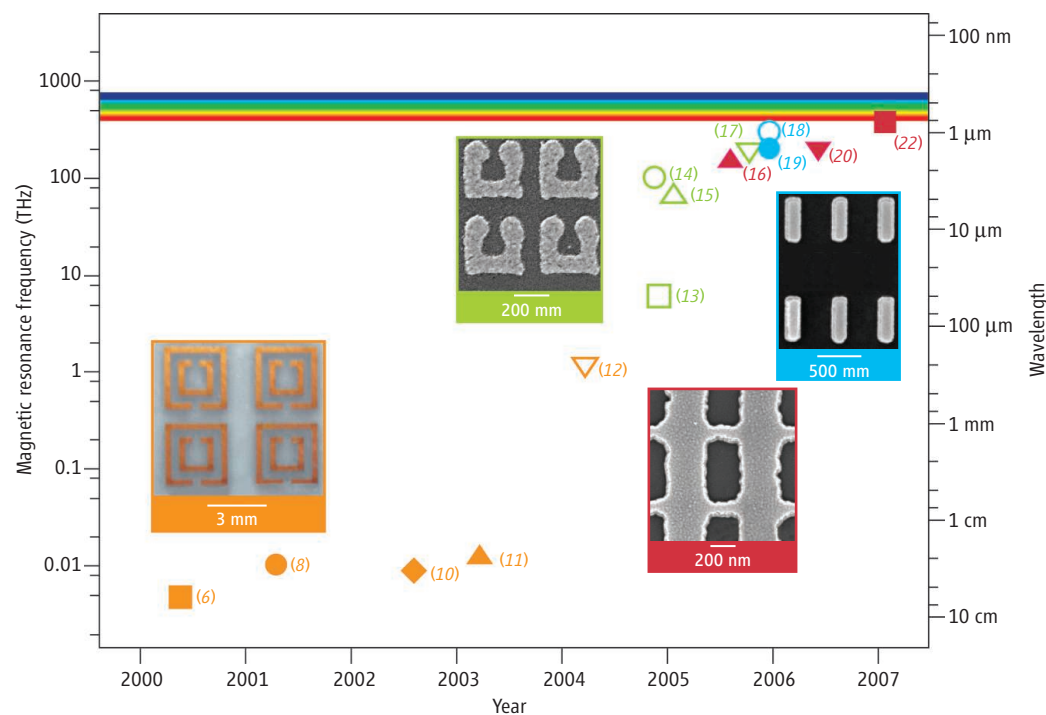
wavelength replace the atoms and molecules of a conventional material, scientists can circumvent this limitation. Metamaterials can be designed to exhibit both electric and magnetic resonances that can be separately tuned to occur in spectra from the low radio-frequency to the visible.

Since the first demonstration (6) of an artificial NIM in 2000, metamaterials have exhibited a broad range of properties and potential applications: nearly zero reflectance; nanometer-scale light sources and focusing; miniaturization of devices, such as antennas and waveguides; and novel devices for medical imaging,

development of the magnetic resonance frequency and/or the frequency of negative n as a function of time. In the early years of the field (2000 to 2003), the design of choice to obtain $\mu < 0$ was an artificial structure proposed by Pendry, the so-called split-ring resonator (SRR). This structure exhibits a band of negative μ values even though it is made of non-magnetic materials. A double SRR is shown at the lower left of the figure. A negative μ at 10 GHz requires SRR dimensions on the order of 1 mm. To obtain negative ϵ , one needs to arrange long and thin wires in a simple cubic lattice, so as to mimic the response of a metal

single SRR took place (see the figure). Indeed, this approach works up to about 200 THz. Unfortunately, it was found that this scaling breaks down for yet higher frequencies for the single SRR. The reason is that the metal of which the SRR is composed starts to strongly deviate from an ideal conductor.

Although these developments have been important proofs of principle, progress was hindered by several experimental details. For example, the combination of these SRRs with metal wires to form a three-dimensional structure is very challenging on the nanometer scale. Thus, there was a hunt for alternative designs that are more suitable for the terahertz or even for the visible regime. The key idea to make this possible was independently realized and published by three different groups in 2005 (16, 18, 19). These designs all show that pairs of metal wires or metal plates, separated by a dielectric spacer, can provide the magnetic resonance. The magnetic resonance originated from the antiparallel current in the wire pair with an opposite sign charge accumulating at the corresponding ends. This resonance provides $\mu < 0$. In addition, an electric resonance with $\epsilon < 0$ results for excitation of a parallel current oscillation. In the transmission measurements, the EM waves were incident normal to the sample surface. This setup is much simpler than that for conventional SRRs and wires, where the incident EM waves must propagate parallel to the sample surface.



Advances in metamaterials. The solid symbols denote $n < 0$; the open symbols denote $\mu < 0$. Orange: data from structures based on the double split-ring resonator (SRR); green: data from U-shaped SRRs; blue: data from pairs of metallic nanorods; red: data from the “fishnet” structure. The four insets give pictures of fabricated structures in different frequency regions.

especially magnetic resonance imaging. For example, metamaterials may lead to the development of a flat superlens (7) that operates in the visible spectrum, which would offer superior resolution over conventional technology and provide image resolutions much smaller than one wavelength of light.

Subsequent theory and experiment (8–22) confirmed the reality of negative refraction. The development of NIMs at microwave frequencies (6, 8–11) has progressed to the point where scientists and engineers are now vigorously pursuing microwave applications. In contrast, research on NIMs that operate at higher frequencies (12–22) is at an early stage, with issues of material fabrication and characterization still being sorted out.

The figure gives a detailed history of the

to electromagnetic waves—that is, below a frequency called the plasma frequency, ϵ is negative. Negative ϵ at gigahertz frequencies might be obtained with wires a few tens of micrometers in diameter and spaced several millimeters apart. By using an array of SRRs and thin wires in alternating layers, several groups (6, 8–11) showed negative n at gigahertz frequencies.

As can be seen from the figure, a negative μ at terahertz and infrared frequencies was achieved in 2004. The idea underlying that work was that the magnetic resonance frequency of the SRR is inversely proportional to its size. Thus, the concepts from the microwave regime could simply be scaled down to shorter wavelengths. For ease of fabrication, a transition from double SRR to sin-

Overlap (18, 19) of the regions where ϵ and μ are both negative with only wire pairs is difficult, so new designs were needed. One way is to introduce extra continuous wires next to the pairs, or to change the shape of the wires. The best design that has been used in 2005 and 2006 is the so-called “double-fishnet” structure, which consists of a pair of metal fishnets separated by a dielectric spacer. This design is shown in the lower right of the figure. Although the choice of the metal constituting the structure is not critical in the microwave regime, it is crucial in the optical and the visible regime because the metamaterial losses are dominated by metal losses. Silver exhibits the lowest losses at optical frequencies, and indeed, going from gold (16, 18, 20) to silver drastically reduced the losses at similar fre-

quencies (21). A suitable measure for the losses is the figure of merit (FOM), defined as the negative ratio of the real to the imaginary part of n . Dolling *et al.* (21) obtained FOM = 3 at a wavelength of 1400 nm, which compares to FOM < 1 for other groups (16, 19, 20). Furthermore, the use of silver has enabled the first negative-index metamaterials at the red end of the visible spectrum (22) (wavelength 780 nm). Another group has also reported a negative n (23, 24), but this has been questioned recently (25).

Only 6 years after their first demonstration, negative-index metamaterials have been brought from microwave frequencies toward the visible regime. However, for applications to come within reach, several goals need to be achieved: reduction of losses (by using crystalline metals and/or by introducing optically amplifying materials), three-dimensional rather than planar struc-

tures, isotropic designs, and ways of mass production of large-area structures. With emerging techniques such as microcontact printing, nanoembossing, holographic lithography, and quantum tailoring of large molecules, it seems likely that these technical challenges can be successfully met. The spirit of metamaterials is to design materials with new and unusual optical properties. In that enterprise, only our imagination and creativity set the limits.

References and Notes

1. D. R. Smith, J. B. Pendry, M. C. K. Wiltshire, *Science* **305**, 788 (2004).
2. D. R. Smith, J. B. Pendry, *Phys. Today* (June 2004), p. 37.
3. C. M. Soukoulis, *Opt. Phot. News* (June 2006), p. 16.
4. C. M. Soukoulis, M. Kafesaki, E. N. Economou, *Adv. Mater.* **18**, 1941 (2006).
5. V. G. Veselago, *Sov. Phys. Uspekhi* **10**, 509 (1968).
6. D. R. Smith *et al.*, *Phys. Rev. Lett.* **84**, 4184 (2000).
7. J. B. Pendry, *Phys. Rev. Lett.* **85**, 3966 (2000).
8. R. A. Shelby, D. R. Smith, S. Schultz, *Science* **292**, 77 (2001).

9. C. G. Parazzoli *et al.*, *Phys. Rev. Lett.* **90**, 107401 (2003).
10. M. Bayindir *et al.*, *Appl. Phys. Lett.* **81**, 120 (2002).
11. R. B. Gregor *et al.*, *Appl. Phys. Lett.* **82**, 2356 (2003).
12. T. J. Yen *et al.*, *Science* **303**, 1494 (2004).
13. N. Katsarakis *et al.*, *Opt. Lett.* **30**, 1348 (2005).
14. S. Linden *et al.*, *Science* **306**, 1351 (2004).
15. S. Zhang *et al.*, *Phys. Rev. Lett.* **94**, 037402 (2005).
16. S. Zhang *et al.*, *Phys. Rev. Lett.* **95**, 137404 (2005).
17. C. Enkrich *et al.*, *Phys. Rev. Lett.* **95**, 203901 (2005).
18. G. Dolling *et al.*, *Opt. Lett.* **30**, 3198 (2005).
19. V. M. Shalaev *et al.*, *Opt. Lett.* **30**, 3356 (2005).
20. G. Dolling, C. Enkrich, M. Wegener, C. M. Soukoulis, S. Linden, *Science* **312**, 892 (2006).
21. G. Dolling *et al.*, *Opt. Lett.* **31**, 1800 (2006).
22. G. Dolling *et al.*, *Opt. Lett.* **32**, 53 (2007).
23. A. N. Grigorenko *et al.*, *Nature* **438**, 335 (2005).
24. A. N. Grigorenko, *Opt. Lett.* **31**, 2483 (2006).
25. A. V. Kildishev *et al.*, <http://arxiv.org/abs/physics/0609234> (2006).
26. We thank Th. Koschny and J. Zhou for preparing the figure. Supported by Ames Laboratory, operated by Iowa State University under contract W-7405-Eng-82 (C.M.S.), and by Helmholtz-Hochschul-Nachwuchsgruppe grant VH-NG-232 (S.L.).

10.1126/science.1136481

ECOLOGY

The Heartbreak of Adapting to Global Warming

Tobias Wang and Johannes Overgaard

Climatic changes have been linked to altered geographical distributions of many organisms, including marine fish (1, 2). Yet, it remains difficult to distinguish direct causal relations between environmental temperature and species distribution patterns (3) from indirect effects through interactions with prey, predators, pathogens, or competitors (4). An ambitious goal of integrative biology is to understand how temperature affects physiological mechanisms at all levels of biological organization. This could allow predictions of how global warming affects animal performance and population dynamics. Animal physiologists commonly rely on laboratory studies to predict temperature tolerance of animals, but whole-animal performance in natural settings is rarely investigated. On page 95 of this issue, Pörtner and Kunst (5) provide compelling evidence that thermal constraints on oxygen transport are causing the population of a marine fish, the viviparous eelpout (*Zoarces viviparus*), to decline in the Wadden Sea.

T. Wang is in the Department of Zoophysiology, Aarhus University, 8000 Aarhus, Denmark. E-mail: tobias.wang@biology.au.dk. J. Overgaard is at the National Environmental Research Institute, Department of Terrestrial Ecology, 8600, Silkeborg, Denmark.

Over the past decade, Pörtner and co-workers have studied various aspects of oxygen transport and metabolism in numerous animal species, including the viviparous eelpout (6). They have identified the pejus temperature (pejus means “turning worse”), beyond which the ability of animals to increase aerobic metabolism is reduced. This reduction is evident from the decline in aerobic scope, which is defined as the proportional difference between resting and maximal rates of oxygen consumption. The temperature range between the lower and higher

Thermal limits. Beyond the “pejus” temperature (T_p), the cardiorespiratory system of the fish can no longer ensure sufficient aerobic scope to sustain reproduction and growth; eventually, activity (T_c) and survival (T_d) are also compromised. These thermal limits are plastic and amenable to the thermal history (acclimatization) of the animals (top three panels). Pörtner and Kunst show that summer temperatures above the pejus cause the population of the European eelpout to decline, indicating that global warming may take effect well before the lethal thermal limits (T_d) are reached (bottom panel).

Laboratory studies of basic physiological constraints on the cardiorespiratory system can be used to predict the impact of global warming on fish.

